

PAPER • OPEN ACCESS

Modelling and Optimal Design of Thick-Walled Composite Pipes under In-Service Conditions

To cite this article: T Wang *et al* 2020 *IOP Conf. Ser.: Mater. Sci. Eng.* **936** 012046

View the [article online](#) for updates and enhancements.

239th ECS Meeting

with the 18th International Meeting on Chemical Sensors (IMCS)

ABSTRACT DEADLINE: DECEMBER 4, 2020



May 30-June 3, 2021

SUBMIT NOW →

Modelling and Optimal Design of Thick-Walled Composite Pipes under In-Service Conditions

T Wang, O Menshykov*, M Menshykova and I A Guz

School of Engineering, University of Aberdeen, AB24 3UE, Scotland, UK

*o.menshykov@abdn.ac.uk

Abstract. The current study is focused on the stress-strain analysis of multi-layered thick-walled fibre reinforced composite pipes under torsional load. Three-dimensional elasticity solution has been obtained and Finite Element Method model has been developed to predict the stress-strain distribution and compute the Tsai-Hill failure coefficients. The models have been validated by comparing with the results available in the literature. As a numerical example the composite pipe subjected to pure torsion load has been considered. The effects of the torque magnitude and layers' thickness for specific pipe lay-ups have been investigated, and the appropriate engineering conclusions and design suggestions have been reported.

1. Introduction

Composite materials were introduced to a range of technical applications over the last decades. Due to their outstanding specific stiffness, strength, lightweight, and chemical resistance, the composite products are applied in aerospace, automotive, military, energy, civil and subsea industries as replacements of the traditional engineering materials (such as metals and alloys). With the increasing customer demands, the composite materials science and manufacturing techniques have been continuously developing and improving [1, 2].

Currently the modelling and design of reinforced composite structures is one of the most dynamically developing branches of structural engineering and materials science because of the variety of in-service loading conditions, component shapes and material combinations (in particular, fibre volume ratios, angles of reinforcement and the appropriate stacking sequences, etc.). The special attention is paid to composite pipes, rods and liners under pressure, bending, torsion and axial loading.

Because of obvious reasons, the most frequently considered type of the loading conditions for pipes is pressure (internal and external). In [3, 4] three-dimensional elasticity method was applied to compute the stress distribution in composite pipes under pressure. Tsai-Hill failure criterion was used for failure prediction. The detailed analysis of failure coefficients along radial direction for different fibre orientations was presented in [4].

Some experiments on filament wound composite pipes were performed in [5, 6]. In the papers the fatigue failure was analysed for the pipes subjected to internal pressure. The whitening, leakage and final pipes' failure were clearly presented. Pipes with surface cracks under inner pressure were considered in [7, 8], where the fatigue was investigated.

The studies of layered composite pipes subjected to inner pressure and thermomechanical loading were published in [9, 10], where the developed three-dimensional anisotropic elasticity method was applied to compute the thermal stress and deformations. With the improvement of computational technics, the thermoplastic composite pipes under pressure and thermomechanical load were studied by Computer-Aided Engineering simulation software [11, 12]. Finite Element Analysis (FEA) results were validated by the available analytical solutions, the detailed through-thickness temperature distributions, and failure coefficients for different stacking sequences were presented and analysed.



The composite pipe subjected to the bending load were investigated in [13–15]. Xia, Takayanagi and Kemmochi [13] presented elasticity solution using the equilibrium equations and the boundary and interface conditions, and analysed the appropriate stresses and strains. Their approach was further developed and utilised by Menshykova and Guz [14], who focused on the distribution of failure coefficients for multi-layered pipes with specific lay-ups. The effects of winding angle on the radial, hoop and axial stress distributions through the wall thickness were also presented. Finally, the computation model of stress distribution and failure coefficients of pipes subjected to combined loading was presented in [15].

Considering the emerging applications of composite cylindrical structures (rods and pipes) in the energy generation and automotive industries (e.g., wind turbine towers and driveshafts), and for the sake of presentation of the current study, here we will present the analytical solution and 3D FEA results for composite pipes under torsion load only. The Tsai-Hill failure criterion will be applied to compute the failure coefficients, predict the pipe failure and formulate the design recommendations.

2. Problem statement

2.1. Stress analysis

The distribution of stresses and strains for each layer of the composite pipe (Figure 1) are given by the following matrix system [3, 4, 16]:

$$\begin{Bmatrix} \sigma_z \\ \sigma_\theta \\ \sigma_r \\ \tau_{\theta r} \\ \tau_{zr} \\ \tau_{z\theta} \end{Bmatrix}^{(l)} = \bar{C} \begin{Bmatrix} \varepsilon_z \\ \varepsilon_\theta \\ \varepsilon_r \\ \gamma_{\theta r} \\ \gamma_{zr} \\ \gamma_{z\theta} \end{Bmatrix}^{(l)} \quad (1)$$

where \bar{C} is the matrix of off-axis stiffness constants.

The radial, hoop, and axial displacements depend on spatial coordinates.

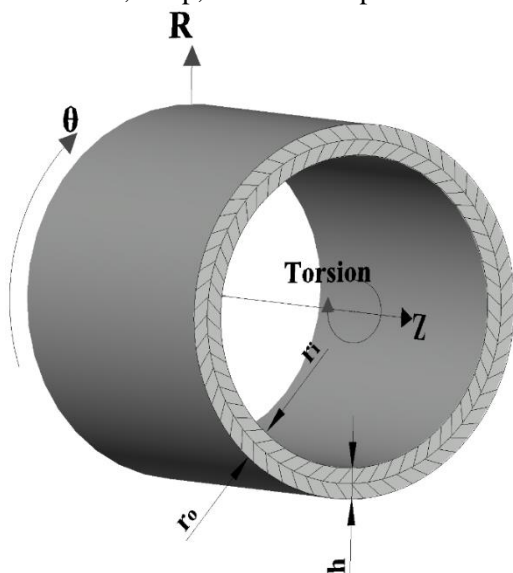


Figure 1. FE model.

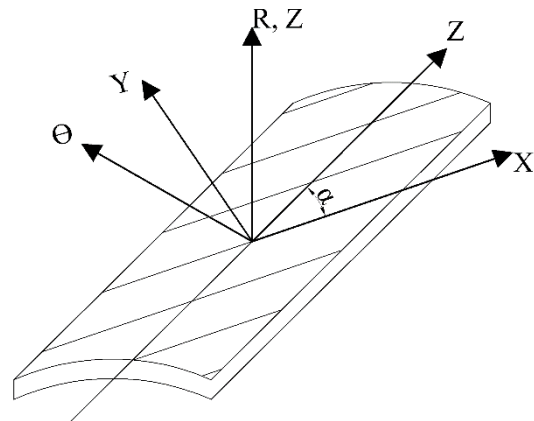


Figure 2. Coordinate systems.

The strains can be calculated from the appropriate displacements as [3, 4]:

$$\varepsilon_r^{(l)} = \frac{du_r^{(l)}}{dr}, \varepsilon_\theta^{(l)} = \frac{u_r^{(l)}}{r}, \varepsilon_z^{(l)} = \varepsilon_0, \quad (2)$$

$$\gamma_{zr}^{(l)} = 0, \gamma_{\theta r}^{(l)} = 0, \gamma_{z\theta}^{(l)} = \gamma_0 r, \quad (3)$$

here γ_0 is the twist of pipe per unit length and ε_0 is the total axial strain.

The equilibrium equations for axisymmetric composite pipe are presented as in [3, 16]:

$$\begin{aligned}\frac{d\sigma_r^{(l)}}{dr} + \frac{\sigma_r^{(l)} - \sigma_\theta^{(l)}}{r} &= 0, \\ \frac{d\tau_{\theta r}^{(l)}}{dr} + \frac{2\tau_{\theta r}^{(l)}}{r} &= 0, \\ \frac{d\tau_{zr}^{(l)}}{dr} + \frac{\tau_{zr}^{(l)}}{r} &= 0.\end{aligned}\quad (4)$$

The boundary conditions under pure torsion load are expressed as

$$\begin{aligned}\sigma_r^{(1)}(r_i) &= 0, \\ \sigma_r^{(N)}(r_o) &= 0, \\ \tau_{\theta r}^{(1)}(r_i) &= \tau_{zr}^{(1)}(r_i) = 0, \\ \tau_{\theta r}^{(N)}(r_o) &= \tau_{zr}^{(N)}(r_o) = 0,\end{aligned}\quad (5)$$

where r_i is the inner radius and r_o is the outer radius of the pipe consisting of N layers.

For the perfectly bonded layers (as we assumed in the current study), the continuity conditions for stresses and displacements must be satisfied. The radial displacements as well as radial and shear stresses must coincide at the interfaces between layers.

$$\begin{aligned}\sigma_r^{(l)}(r_l) &= \sigma_r^{(l+1)}(r_l), \\ u_r^{(l)}(r_l) &= u_r^{(l+1)}(r_l), \\ \tau_{\theta r}^{(l)}(r_l) &= \tau_{\theta r}^{(l+1)}(r_l).\end{aligned}\quad (6)$$

Furthermore, by integrating the moment of the shear stress $\tau_{z\theta}$ over the cross-sectional area one may derive the following integral equation [3, 16]:

$$2\pi \sum_{l=1}^N \int_{r_{l-1}}^{r_l} \tau_{z\theta}^{(l)}(r) r^2 dr = T, \quad (7)$$

where T is the torque.

The integral equation for axial force is the following [3, 16]:

$$2\pi \sum_{l=1}^N \int_{r_{l-1}}^{r_l} \sigma_z^{(l)}(r) r dr = 0. \quad (8)$$

From equation (1)–(4) the radial displacement can be written as [3]:

$$u_r^{(l)} = A^{(l)} r^{\beta^{(l)}} + B^{(l)} r^{-\beta^{(l)}} + \alpha_1^{(l)} \varepsilon_0 r + \alpha_2^{(l)} \gamma_0 r^2, \quad (9)$$

where $A^{(l)}$ and $B^{(l)}$ are unknown integration constants and

$$\beta^{(l)} = \left(\frac{\bar{C}_{22}^{(l)}}{\bar{C}_{33}^{(l)}} \right)^{\frac{1}{2}}, \quad \alpha_1^{(l)} = \frac{\bar{C}_{12}^{(l)} - \bar{C}_{13}^{(l)}}{\bar{C}_{33}^{(l)} - \bar{C}_{22}^{(l)}}, \quad \alpha_2^{(l)} = \frac{\bar{C}_{26}^{(l)} - 2\bar{C}_{36}^{(l)}}{4\bar{C}_{33}^{(l)} - \bar{C}_{22}^{(l)}}. \quad (10)$$

The transformed strains can be calculated as [3]:

$$\{\varepsilon\} = \begin{Bmatrix} \varepsilon_1 \\ \varepsilon_2 \\ \varepsilon_3 \\ \gamma_{23} \\ \gamma_{13} \\ \gamma_{12} \end{Bmatrix} = \begin{bmatrix} \cos\alpha^2 & \sin\alpha^2 & 0 & 0 & 0 & \cos\alpha\sin\alpha \\ \sin\alpha^2 & \cos\alpha^2 & 0 & 0 & 0 & -\cos\alpha\sin\alpha \\ 0 & 0 & 1 & 0 & 0 & 0 \\ 0 & 0 & 0 & \cos\alpha & -\sin\alpha & 0 \\ 0 & 0 & 0 & \sin\alpha & \cos\alpha & 0 \\ -2\cos\alpha\sin\alpha & 2\cos\alpha\sin\alpha & 0 & 0 & 0 & \cos\alpha^2 - \sin\alpha^2 \end{bmatrix} \begin{Bmatrix} \varepsilon_z \\ \varepsilon_\theta \\ \varepsilon_r \\ \gamma_{\theta r} \\ \gamma_{zr} \\ \gamma_{z\theta} \end{Bmatrix}, \quad (11)$$

$$\{\varepsilon\} = [T_\varepsilon] \{\bar{\varepsilon}\}$$

where α is the winding angle, $\bar{\varepsilon}$ is the strain vector in the off-axis coordinate system (Figure 2).

The relation between off-axis and on-axis stiffness constants is the follow:

$$\left[\bar{C}_{ij}^{(k)} \right] = [T_\varepsilon]^T \left[C_{ij}^{(k)} \right] [T_\varepsilon] \quad (12)$$

Consequently, $\left\{ \bar{C}_{ij}^{(k)} \right\} = [A] \left\{ C_{ij}^{(k)} \right\}$, where $[A]$ is the transformation matrix of \sin and \cos [3].

Substituting expressions for displacements and stresses into boundary and continuity conditions and integral equations for axial force (8) and torque (7) one may obtain the system of algebraic equations and consequently find the unknown constants and stresses in the pipe.

2.2. Tsai-Hill failure criterion

The failure coefficients are computed using the following stresses in principal material directions

$$\begin{bmatrix} \sigma_x \\ \sigma_y \\ \tau \end{bmatrix} = \begin{bmatrix} \cos^2 \alpha & \sin^2 \alpha & 2\cos\alpha\sin\alpha \\ \sin^2 \alpha & \cos^2 \alpha & -2\cos\alpha\sin\alpha \\ -\cos\alpha\sin\alpha & \cos\alpha\sin\alpha & \cos^2 \alpha - \sin^2 \alpha \end{bmatrix} \begin{bmatrix} \sigma_z \\ \sigma_\theta \\ \tau_{z\theta} \end{bmatrix} \quad (13)$$

The Tsai-Hill failure coefficient is [4]

$$\text{Failure Coefficient} = \frac{\sigma_x^2}{X_T^2} - \frac{\sigma_x\sigma_y}{X_T^2} + \frac{\sigma_y^2}{Y_T^2} + \frac{\tau^2}{S^2}, \quad (14)$$

where X_T and Y_T are longitudinal and transversal tensile strength values, and S is the shear strength. The failure happens when the failure coefficient becomes greater than 1.

3. Case studies

3.1. 3D Finite Element modelling

Abaqus/CAE 2019 was used to develop a numerical model in order to calculate stresses in a section of thick-walled composite pipe under torsion load. All layers are assumed to be perfectly bonded. Carbon/epoxy fibre composite (T300/LY5052) was considered in this study, and T300/5208 composite was used for validation. The material properties are shown in Table 1.

Table 1. Material properties [4, 16].

Properties	T300/LY5052	T300/5208
E_1 (GPa)	135	132
E_2 (GPa)	8	10.8
G_{12} (GPa)	3.8	5.65
ν_{12}	0.27	0.24
ν_{23}	0.49	0.59
X_T (MPa)	1860	1513
Y_T (MPa)	76	43.4
S (MPa)	98	86.87

The torque was applied and the rigid body constraints were used. The model was meshed using Abaqus C3D20R elements (quadratic brick elements with reduced integration).

3.2. Validation

To validate the results, obtained by developed analytical and numerical models, we compared them with the one presented in Herakovich [16]. Two-layer composite pipe with the ply sequence $[\pm 45^\circ]$ was modelled, and the distributions of the stresses in the pipe wall were computed and normalised for comparison.

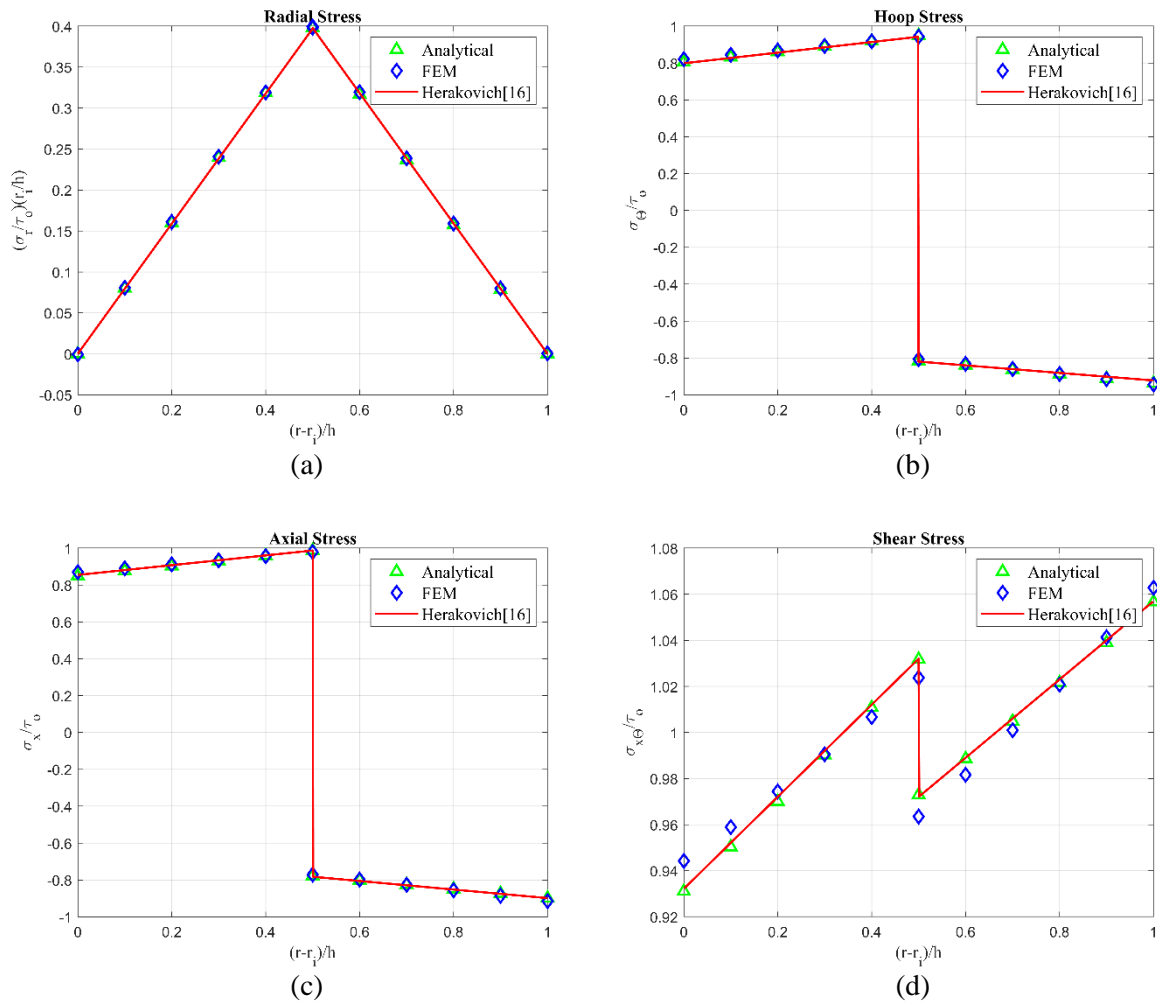


Figure 3. Radial (a) hoop (b) axial (c) shear (d) normalised stress values vs. normalised radius.

The average axial stress σ_o is

$$\sigma_o = \frac{P_x}{\pi(r_o^2 - r_i^2)}, \quad (15)$$

and the average shear stress τ_o is

$$\tau_o = \frac{3T_x}{2\pi(r_o^3 - r_i^3)}. \quad (16)$$

In this study $r_i/h = 5$ (where h is the total thickness of the composite structure) and the magnitude of the torque is $1kNm$.

Figure 3 shows that the analytical and numerical results coincide with the model ones [16].

3.3. Numerical results

In this section, we computed the failure coefficients for the four-layer composite pipe subjected to torques of different magnitude.

Inner and outer radii were $30mm$ and $36mm$, respectively, and the layer thickness was $1.5mm$.

The failure coefficients for the composite pipe $[\pm 55^\circ/\pm 60^\circ]$ for a range of torques from 5 to $30kNm$ are presented in Figure 4.

Failure coefficient clearly rises with the rise of the torque magnitude and the failure happens when the torque exceeds $20kNm$.

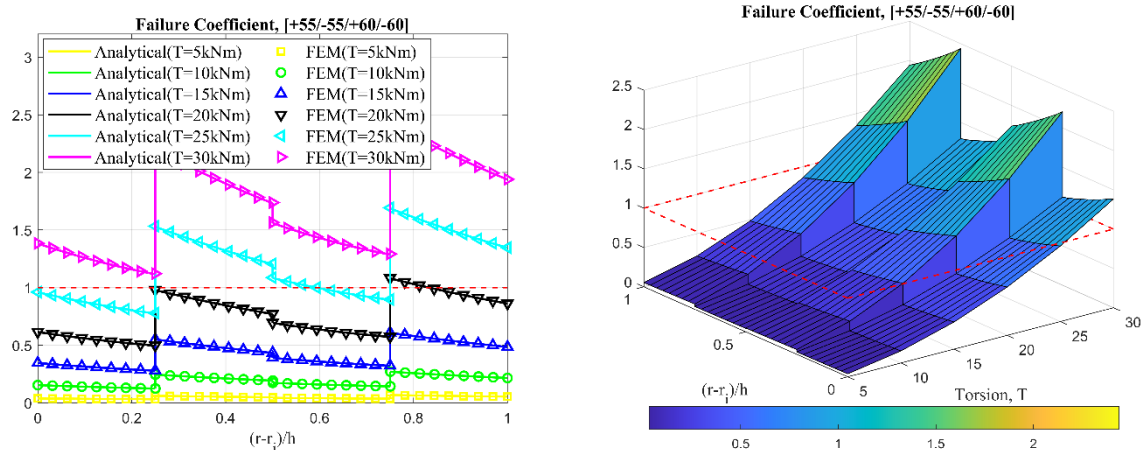


Figure 4. The failure coefficients for composite pipes subjected to torque.

4. Conclusions

Multi-layered long fibre reinforced composite pipes under torque load were investigated. Numerical and analytical results were validated by comparing with the model one presented in Herakovich [16]. Comparison of numerical results with the analytical ones was carried out for the pipes of different lay-ups subjected to the range of torsional load. That would be beneficial for the future analysis to investigate the interlaminar crack behaviour in thick walled composite pipes under different types of load [18].

5. References

- [1] Yu K, Morozov E V, Ashraf M A and Shankar K 2017 A review of the design and analysis of reinforced thermoplastic pipes for offshore applications *J. Reinf. Plast. Compos.* **36** 1514–30
- [2] Rafiee R 2016 On the mechanical performance of glass-fibre-reinforced thermosetting-resin pipes: A review *Compos. Struct.* **143** 151–64
- [3] Xia M, Takayanagi H and Kemmochi K 2001 Analysis of multi-layered filament-wound composite pipes under internal pressure *Compos. Struct.* **53** 483–91
- [4] Guz I A, Menshykova M and Paik J K 2017 Thick-walled composite tubes for offshore applications: an example of stress and failure analysis for filament-wound multi-layered pipes *Ships Offshore Struct.* **12** 304–22
- [5] Tarakçioğlu N, Gemi L and Yapici A 2005 Fatigue failure behavior of glass/epoxy $\pm 55^\circ$ filament wound pipes under internal pressure *Compos. Sci. Technol.* **65** 703–8
- [6] Gemi L, Tarakçioğlu N, Akdemir A and Şahin Ö S 2009 Progressive fatigue failure behavior of glass/epoxy $(\pm 75^\circ)_2$ filament-wound pipes under pure internal pressure *Mater. Des.* **30** 4293–8
- [7] Tarakcioglu N, Samanci A, Arikan H and Akdemir A 2007 The fatigue behavior of $(\pm 55^\circ)_3$ filament wound GRP pipes with a surface crack under internal pressure *Compos. Struct.* **80** 207–11
- [8] Arikan H 2010 Failure analysis of $(\pm 55^\circ)_3$ filament wound composite pipes with an inclined surface crack under static internal pressure *Compos. Struct.* **92** 182–7
- [9] Bakaiyan H, Hosseini H and Ameri E 2009 Analysis of multi-layered filament-wound composite pipes under combined internal pressure and thermomechanical loading with thermal variations *Compos. Struct.* **88** 532–41
- [10] Xia M, Kemmochi K and Takayanagi H 2001 Analysis of filament-wound fiber-reinforced sandwich pipe under combined internal pressure and thermomechanical loading *Compos. Struct.* **51** 273–83
- [11] Hastie J C, Kashtalyan M and Guz I A 2019 Failure analysis of thermoplastic composite pipe (TCP) under combined pressure, tension and thermal gradient for an offshore riser application *Int. J. Press. Vessel. Pip.* **178** 103998
- [12] Hastie J C, Guz I A and Kashtalyan M 2019 Effects of thermal gradient on failure of a thermoplastic composite pipe (TCP) riser leg *Int. J. Press. Vessel. Pip.* **172** 90–9

- [13] Xia M, Takayanagi H and Kemmochi K 2002 Bending behavior of filament-wound fiber-reinforced sandwich pipes *Compos. Struct.* **56** 201–10
- [14] Menshykova M and Guz I A 2014 Stress analysis of layered thick-walled composite pipes subjected to bending loading *Int. J. Mech. Sci.* **88** 289–99
- [15] Cox K, Menshykova M, Menshykov O and Guz I A 2019 Analysis of flexible composites for coiled tubing applications *Compos. Struct.* **225** 111118
- [16] Herakovich C T 1998 *Mechanics of Fibrous Composites* (New York: John Wiley)
- [17] Cagdas I U 2017 Optimal design of variable stiffness laminated composite truncated cones under lateral external pressure *Ocean Eng.* **145** 268–76
- [18] Menshykova M V, Menshykov O V, Guz I A 2009 Linear interface crack under plane shear wave *CMES – Comp. Model. Eng.* **48(2)** 107–20